Region of Interest Detection in Dermoscopic Images for Natural Data-augmentation

Manu Goyal, Saeed Hassanpour , Moi Hoon Yap, *Member, IEEE*

Abstract—With the rapid growth of medical imaging research, there is a great interest in the automated detection of skin lesions with computer algorithms. The state-of-the-art datasets for skin lesions are often accompanied with very limited amount of ground truth labeling as it is laborious and expensive. The Region Of Interest (ROI) detection is vital to locate the lesion accurately and must be robust to subtle features of different skin lesion types. In this work, we propose the use of two object localization meta-architectures for end-to-end ROI skin lesion detection in dermoscopic images. We trained the Faster-RCNN-InceptionV2 and SSD-InceptionV2 on the ISBI-2017 training dataset and evaluated their performance on the ISBI-2017 testing set, PH2 and HAM10000 datasets. Since there was no earlier work in ROI detection for skin lesion with CNNs, we compared the performance of skin localization methods with the state-of-the-art segmentation method. The localization methods proved superior to the segmentation method in ROI detection on skin lesion datasets. In addition, based on the detected ROI, an automated natural data-augmentation method is proposed and used as pre-processing in the lesion diagnosis and segmentation task. To further demonstrate the potential of our work, we developed a real-time smart-phone application for automated skin lesions detection.

Index Terms—Skin Cancer, Deep Convolutional Neural Networks, Natural Data-augmentation, ROI detection, Smart-phone Application

I. INTRODUCTION

ACCORDING to the Skin Cancer Foundation [1], the incidence of new skin cancers is greater than the combined new cancer cases for breast, lung, colon, and prostate over the past three decades. In current medical practice, dermatologists primarily examine the patients by visual inspection with a dermatoscope to determine the condition of skin lesions. Relying on self-vigilance and medical examination by human vision risks life and survival rate as it is difficult to identify the type of skin lesions by naked eyes. Dermoscopy is a non-invasive imaging that allows visualization of the skin surface by using a light magnifying device and immersion fluid [2]. It is one of the most widely used imaging techniques in dermatology, and it has increased the diagnosis rate [3].

The previous state-of-the-art computer-aided diagnosis on dermoscopic images composed of multi-stages, which include image pre-processing, image segmentation [4], feature extraction [5] and classification [6]. Since, the introduction of one

M. Goyal is with Department of Biomedical Data Science, Dartmouth College, Hanover, NH, USA (e-mail: m.goyal@mmu.ac.uk)

S.Hassanpour is with Departments of Biomedical Data Science, Computer Science, and Epidemiology, Dartmouth College, Hanover, NH, USA.

M.H. Yap are with the School of Computing, Mathematics and Digital Technology, Manchester Metropolitan University, John Dalton Building, M1 5GD, Manchester, UK.

of the largest public skin lesion dataset as ISIC forum and ISIC yearly skin lesion challenge, end-to-end deep learning algorithms has widely gained popularity for the skin lesion classification and segmentation [7]. In 2017, International Skin Imaging Collaboration conducted the ISBI challenge to get the best performance measures for skin lesion classification and segmentation in which participant team named Recod Titans won the binary classification to detect melanoma with AUC score of 0.874 and Yading Yuan won the segmentation challenge with a score of 0.765 in *Jaccard Similarity Index (JSI)* [8].

Region Of Interest (ROI) detection was shown to be important in medical image analysis [9], [10], [11], where it is defined as a bounding box circumscribing the lesion. This paper focuses on the automatic detection of the ROI in dermoscopic images. There are different types of skin lesions such as naevus, melanoma, and seborrhoeic keratoses which have large intra-class variations in terms of color, size, place, and appearance for each class and high inter-class visual similarities [12]. Hence, the detected ROI can help classification algorithms to learn more precise features for classifying different lesion types. In addition, researchers augmented the data by using image manipulation techniques to overcome the lack of training data in deep learning. Tschandl et al. [13] used different magnifications and angles of the skin lesions to produce natural data-augmentation for HAM10000 dataset. However, it means laborious processing and redundant data for the same skin lesion. With the aid of our ROI detection, this can be done automatically. Hence, automated ROI detection for skin lesions has great potential in improving the quality of the dataset, the accuracy of lesion localization and reducing the laborious process of manual annotation. In this experiment, we could not compare our proposed deep learning localization methods with state-of-the-art traditional machine learning algorithms for skin lesion localization as there would be a need of producing expert annotations of large skin lesion datasets according to their methods. The key contributions of this paper include:

1) We propose the use of CNNs for ROI detection on dermoscopic images of the ISIC Challenge 2017 dataset. Then, we test the robustness of trained models on other completely unseen publicly available datasets, i.e. PH2 and HAM10000 datasets.
2) We demonstrate the use of the localization algorithm to produce natural data-augmentation. We tested the performance of deep learning algorithms with the use of natural data-augmentation as pre-processing for lesion
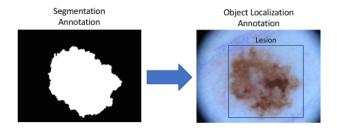
Fig. 1. Conversion of Segmentation annotation to Localization annotation in ISIC Challenge 2017 dataset.

Fig. 2. Convolutions layers of CNN are used to extract the feature maps of skin lesion images. Conv refers to convolutional layers

segmentation and classification.

3) We demonstrate the practical application of this work by developing an android camera app, which utilizes these models in mobile devices for real-time detection and localization of skin lesions. Furthermore, real-time skin lesion detection can be used to capture a highly standardized skin lesion dataset using a smart-phone camera.

II. METHODOLOGY

This section discusses the publicly available skin lesion datasets, the preparation of the ground truth, network hyper-parameters and the performance measures to validate our results.

A. Publicly Available Skin-Lesion Datasets

For this work, we used three publicly available datasets for skin lesions ISBI-2017 Challenge (Henceforth ISBI-2017), PH2 and HAM10000. PH2 has 200 images in which 160 images are naevus (atypical naevus and common naevus), and 40 images are of melanoma [14]. ISBI-2017 is a subset of ISIC Archive dataset [8]. In the segmentation category, it consists of 2750 images with 2000 images in the training set, 150 in the validation set and 600 in the testing set. Since the ground truths for the challenges only included the segmentation mask, to produce the ground truth for ROI, we circumscribed a rectangle bounding box on the segmentation mask as shown in Fig. 1. We solely used ISBI-2017 to train the models. HAM10000 is a collection of 11,788 dermoscopic images of different skin lesions collected from multiple sources around the world [13]. We resized all the images to 500×375 to improve the performance and reduce the computational costs.

B. Deep Learning Methods for ROI Detection

We used the Tensorflow object detection API [15] that provides an open source framework that makes it very convenient to design and build various object localization models.

The Faster RCNN [16] is a region proposal network with three steps to provide faster and accurate box proposals and classify them as an object or background. First, CNN is used to extract the convolutional features from the input image. Second, box proposals of different aspects are generated based on the features. Finally, box proposals are fed to CNN for classification and regression. The classification task predicts
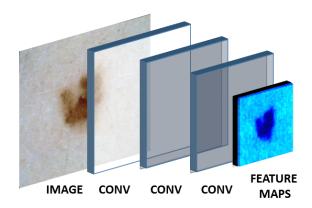
whether the box proposals contain an object or not and regression further improves the location of box proposals.

Single Shot Multibox Detector (SSD) [17] is a recent meta-architecture for the object localization which uses a single stage convolutional neural network to predict classes directly and anchor offsets without the need of a third stage as used in Faster-RCNN [16]. The SSD meta-architecture can produce anchors much faster than other object localization networks which makes it more suitable for the mobile platforms which have limited resources than computers.

For this work, we propose the use of InceptionV2 as a base network for feature extractor and classification of anchor boxes with all meta-architectures as mentioned above for the ROI lesions detection. We chose Inception-V2 network as it provides a balanced trade-off between speed and accuracy that is appropriate for the implementation of a smartphone application using these algorithms. In general, the object localization network consists of three stages to produce ROI detection [16]. These stages are briefly explained below:

1) CNN as Feature Extractor: In the first step, the input image goes through a convolution network that outputs a set of convolutional feature maps on the last convolutional layer as shown in Fig. 2. We used Inception-V2 which is a lightweight CNN with new features such as improvement in the normalization and factorizing the large convolution to smaller convolutions to reduce computations. The other added features are using the depth-wise convolution layers rather than normal convolution layers to further improve the processing time and batch normalization layer which can decrease internal covariate shift, also combat the gradient vanishing problem to improve the convergence during training [18].

2) Generation of proposals: In the second stage, a sliding window of 3×3 is run spatially on these feature maps. For each sliding window, a number of proposals are generated which all have the same centerbut with different aspect ratios and scales as shown in Fig. 3. Then, Intersection of Union (IoU) of each proposal is compared with the Ground Truth (GT) of that image to select the proposal for the next stage.

3) Proposals Classification and Regression: The selected proposals from the second stage are classified as an object or background by CNN and refined further to get the final ROI
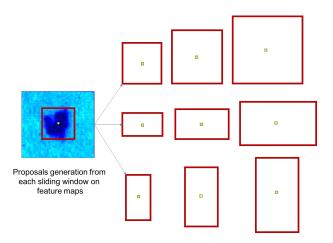
Fig. 3. Proposals of different aspect ratios and scales are generated from the feature maps.

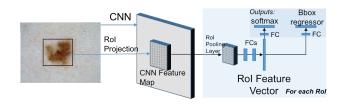detections with the help of regression as shown in Fig. 4.

Fig. 4. Proposals are classified and refined further to get the final ROI detections. Where FC refers to Fully-connected layer.

As there are no existing ROI detection methods by CNN for skin lesion research is available, we compare our results with skin segmentation algorithm. We implemented DeepLabV3+ [19], which is one of the best semantic segmentation networks to train on the ISIC-2017 segmentation dataset. We received state-of-the-art *JSI* Score of 77.15 on the testing set which is better than *JSI* Score achieved by the competition winner [8]. Similar to the way that we generated ground truth, the circumscribed rectangle bounding boxes are generated from the resulted segmentation mask.

C. Quantitative Performance Measures for Lesion Detection

All performance metrics are calculated with "overlap criterion" as an *intersection over union* (*IoU*) of the detected lesion and GT. A *True Positive* (*TP*) is when the $IoU > 0.5$. A *False Positive* (*FP*) is a detected ROI with $IoU \leq 0.5$ and the duplicate bounding boxes. A *False Negative* (*FN*) is when there is no ROI detected by the algorithm.

We evaluate the performance of the proposed methods using three metrics, i.e. *Precision*, *Recall* and *Mean IoU*. The *Precision* is calculated by number of *TP* divided by the sum of number of *TP* and *FP*. The *Recall* is the number of *TP* divided by sum of number of *TP* and *FP*. We also report the *Mean IoU*, which is the average of the overlap percentage of the *TP* cases (detected lesions).

III. EXPERIMENT AND RESULTS

We used ISBI-2017 dataset to train all the networks on a GPU machine with the following specification: (1) Hardware:

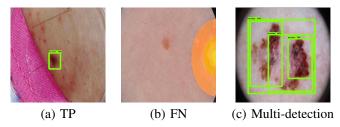(a) TP   (b) FN   (c) Multi-detection

Fig. 5. Examples of rrence Produced by Faster-RCNN-InceptionV2: (a) *TP*: Detection with *IoU* of 98.2%; (b) *FN*: No detection where the model failed to detect the skin lesion; and (c)Multi-detection: The bounding box with highest confidence was selected as the detected ROI. The remaining bounding boxes were counted as *FP*.

CPU - Intel i7-6700 @ 4.00Ghz, GPU - NVIDIA TITAN X 12Gb, RAM - 32GB DDR5 (2) Software: Tensor-flow.

We trained SSD-InceptionV2 for 100 epochs with a batch size of 24, optimizer as `RMS_Prop` with a learning rate of 0.004 and decay factor of 0.95. For transfer-learning, we used the pre-trained model that is trained on the MS-COCO dataset which consists of more than 80000 images of 90 classes [15], [20]. For training of Faster-RCNN-InceptionV2, we used a batch size of 2, `Momentum` optimizer with manual step learning rate with an initial rate as 0.0002 with step-down rate of 10% after every 33 epochs. In Fig. 5, we show the examples of inference produced by the skin localization models. The majority of *FN* cases has very subtle features or similar skin tone or covered with lots of hair. For multi-detection cases, we used the bounding box with the highest confidence for final results. In the case of equal confidence scores, we select the bounding box with the largest area. For each test image, we generate a single bounding box as the detected ROI.

In Table I, we indicate the performance of each trained models on ISBI-2017 testing dataset. Overall, Faster-RCNN-InceptionV2 performed best in regards to the ROI localization, with a *precision* of 0.945 (94.5%), *recall* of 0.943 (94.3%) for $IoU > 0.5$. It performed well throughout the performance indices used for $IoU > 0.75$. The DeepLabV3+ scored first position in *mean IoU(0.5)* performance index due to low score of 0.887 in *precision(0.5)* and *recall(0.5)* . Comparing the SSD-InceptionV2 and DeepLabV3+ performances, SSD-InceptionV2 outperformed DeepLabV3+ in *precision(0.5)* and *recall(0.5)* whereas DeepLabV3+ performed better in *precision(0.5)*, *recall(0.5)* and *mean IoU(0.5&0.75)*.

A. Performance Evaluation on PH2 Dataset and HAM10000 Dataset

In ISBI-2017, the skin lesion types are benign nevi, melanoma and seborrhoeic keratosis. We randomly selected a subset of HAM10000 by picking 50 images each from four categories of skin lesions that are actinic keratosis, basal cell carcinoma, dermatofibroma, vascular lesion other than original categories of skin lesions. We further investigate the performance of these models on PH2 and a subset of HAM10000. Again, Faster-RCNN-InceptionV2 performed better than the other models on these completely unseen datasets as shown in Table II and Table III. Faster-RCNN-InceptionV2 performed very well on PH2 dataset in terms

TABLE I
COMPARISON OF PERFORMANCE FOR DIFFERENT LOCALIZATION AND SEGMENTATION METHODS FOR ROI DETECTION ON ISBI-2017 TESTING SET
WHERE PR REFERS PRECISION.

Method	PR(0.5)	Recall(0.5)	Mean IoU(0.5)	PR(0.75)	Recall(0.75)	Mean IoU(0.75)
FRCNN-Inception-V2	**0.945**	**0.943**	0.811	**0.810**	**0.863**	**0.874**
SSD-Inception-V2	0.918	0.872	0.803	0.603	0.688	0.866
DeepLabV3+	0.887	0.887	**0.816**	0.660	0.738	0.870

of *precision(0.5)* and *recall(0.5)*. Moreover, SSD-InceptionV2 performance was better in most of the performance measures than DeepLabV3+ on these datasets. We reported the curves of performance measures of all proposed methods for the skin lesion localization task in Fig. 6.

IV. NATURAL DATA-AUGMENTATION

In the publicly available dataset of skin lesions, the size of images varies between 540 × 722 and 4499 × 6748. Especially, dermoscopic images have high resolution images as they are captured with a professional camera. On the other hand, most of the deep learning algorithms use smaller image size such as 224×224. For natural data-augmentation, multiple copies of a same skin lesion image are captured with different magnification and angles. Our proposed method can provide the natural data-augmentation technique for dermoscopic images as shown in Fig. 7 without capturing the redundant data and any loss of quality. The number of natural data-augmentation with localization methods depends upon the input image size for algorithm and the ratio between the size of ROI and size of an image. In addition, our methods were able to remove other unwanted artifacts which can confuse the algorithm as illustrated in Fig. 7(a). In Fig. 8, we showed natural data-augmentation with different angles using our proposed methods.

A. Skin Segmentation Results using Natural Data-Augmentation

In this section, we checked the effectiveness of the natural data-augmentation technique as a pre-processing step for the segmentation of skin lesions and compared with the state-of-the-art segmentation algorithms.

We trained DeeplabV3+ for skin lesion segmentation with original ISIC-2017 segmentation dataset images with natural data-augmentation. We used 24356 training and 1792 validation images respectively from original 2000 training and 150 validation images with natural data-augmentation. The inference for the test images is produced as shown in Fig. 9.

In Table IV, we reported performance measures of state-of-the-art segmentation algorithms and our proposed DeeplabV3+ using natural data-augmentation on the ISIC-2017 segmentation dataset. The results showed that the proposed method segmented the skin lesions with *Jaccard index* of 82.3% for the ISBI 2017 test dataset. In comparison to CDNN, U-Net, FCN, SegNet, and DeeplabV3+ the proposed method

(DeeplabV3+ with natural data-augmentation) outperformed them by 5.8%, 6.1%, 8.3%, 12.7%, and 5.2% for the *Jaccard index*, respectively.

1) Lesion Diagnosis with Natural Data-augmentation: We tested ISIC-2017 classification challenge (benign vs malignant) with state-of-the-art deep learning algorithms such as VGG-16, ResNet-50, and Inception-V3 to test the effectiveness of the natural augmentation. We extracted the features from pre-trained models and trained the final layers to get the classification results.

In Table V, we reported the performance of state-of-the-art deep learning algorithms with and without natural data-augmentation for the classification of benign and malignant lesions in the ISIC-2017 testing set. It is clearly evident from Table V, by incorporating the proposed natural data-augmentation method, the performance of deep learning methods is improved by the margin of 5.96% (mean *Accuracy*), 5.66% (mean *Sensitivity*), 6.2% (mean *Specificity*) and 14.34% (mean *MCC score*). Overall, ResNet50 with natural data-augmentation performed best in regards to the lesion diagnosis task, with an *Accuracy* of 0.827 (82.73%), *Sensitivity* of 91.52% and *Specificity* of 46.13%.

V. SMART-PHONE APPLICATION FOR LESION DETECTION

For real-time inference on mobile devices, it is important to consider lightweight models (low latency) in terms of the size of the model and inference speed. We deployed SSD-InceptionV2 for real-time ROI detection on smart-phone using an android studio and TensorFlow mobile library. Since these models were trained on dermoscopic images, we used MoleScope attachment for Samsung A5 smart-phone that provides a high-resolution, detailed view of the moles through magnification and specialized lighting as shown in Fig. 11. We tested 30 different types of skin lesions on 12 different people with this smart-phone application. This application was able to provide accurate real-time detection and localization of skin lesions. It can be a useful feature for data capturing of dermoscopic images with different camera devices.

In Table VI, the size and speed (inference) of our trained localization algorithms are reported. The example of real-time inference of skin lesion detection using our android smartphone application is shown in https://youtu.be/gKQyZ4QeV0U. Additional examples of skin lesion localization are shown in Fig. 10.

TABLE II
COMPARISON OF PERFORMANCE FOR DIFFERENT LOCALIZATION AND SEGMENTATION METHODS FOR ROI DETECTION ON PH2 DATASET. WHERE PR REFERS TO PRECISION

Method	PR(0.5)	Recall(0.5)	Mean IoU(0.5)	PR(0.75)	Recall(0.75)	Mean IoU(0.75)
FRCNN-Inception-V2	**1.000**	**1.000**	**0.901**	**0.960**	**0.960**	**0.912**
SSD-Inception-V2	0.985	0.985	0.889	0.935	0.935	0.901
DeepLabV3+	0.955	0.955	0.885	0.860	0.860	0.912

TABLE III
COMPARISON OF PERFORMANCE FOR DIFFERENT LOCALIZATION AND SEGMENTATION METHODS FOR ROI DETECTION ON A SUBSET OF HAM10000. WHERE PR REFERS TO PRECISION

Method	PR(0.5)	Recall(0.5)	Mean IoU(0.5)	PR(0.75)	Recall(0.75)	Mean IoU(0.75)
FRCNN-InceptionV2	**0.833**	**0.824**	**0.786**	**0.544**	**0.539**	0.849
SSD-InceptionV2	0.808	0.728	0.756	0.423	0.381	0.853
DeepLabV3+	0.695	0.688	0.774	0.415	0.411	**0.870**

TABLE IV
PERFORMANCE EVALUATION OF STATE-OF-THE-ART SEGMENTATION ALGORITHMS AND DEEPLABV3+ WITH NATURAL DATA-AUGMENTATION TRAINED AND TESTED ON ISIC-2017 SEGMENTATION DATASET

Methods	Accuracy	Dice	Jaccard	Sensitivity	Specificity
First: Yading Yuan (CDNN Model) [21]	0.934	0.849	0.765	0.825	0.975
Second: Matt Berseth (U-Net) [22]	0.932	0.847	0.762	0.820	**0.978**
FCN [23]	0.927	0.828	0.736	0.811	0.967
SegNet [24]	0.918	0.821	0.696	0.801	0.954
Mask-RCNN [25]	0.935	0.856	0.774	0.848	0.960
DeeplabV3+ [19]	0.936	0.851	0.771	0.843	0.972
DeeplabV3+ (Natural Data-augmentation)	**0.947**	**0.886**	**0.823**	**0.898**	0.964

TABLE V
PERFORMANCE EVALUATION OF STATE-OF-THE-ART DEEP LEARNING ALGORITHMS ON ISIC-2017 LESION DIAGNOSIS TESTING SET

Methods	Accuracy	Precision	Sensitivity	Specificity	F-1 Score	MCC
VGG-16	0.735	0.832	0.838	0.325	0.835	0.164
Inception-V3	0.745	0.843	0.841	0.350	0.841	0.190
ResNet-50	0.760	0.854	0.847	0.402	0.850	0.245
VGG-16 (Natural Data-augmentation)	0.787	0.857	0.882	0.393	0.870	0.289
Inception-V3 (Natural Data-augmentation)	0.803	0.863	0.899	0.410	0.880	0.332
ResNet-50 (Natural Data-augmentation)	**0.827**	**0.875**	**0.915**	**0.461**	**0.895**	**0.408**

TABLE VI
COMPARISON OF LATENCY OF DEEP LEARNING LOCALIZATION MODELS

Model Name	Size of Model(MB)	Average Speed(ms)
SSD-InceptionV2	47.6	38
Faster-RCNN-InceptionV2	58.6	57
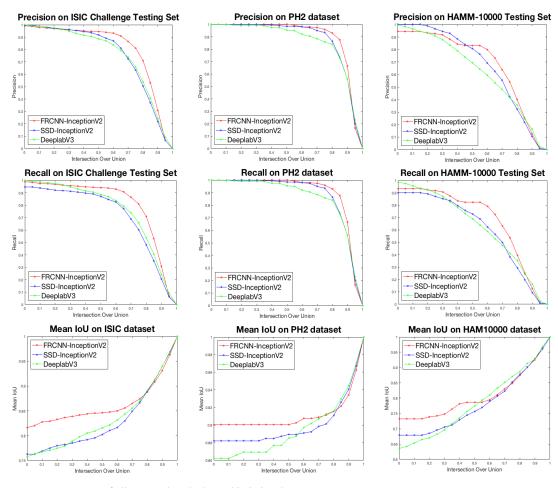
Fig. 6. Performance measure curves of all proposed methods on skin lesion datasets

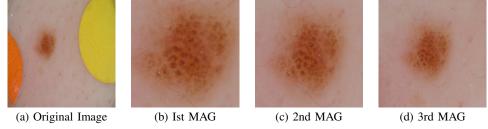(a) Original Image   (b) Ist MAG   (c) 2nd MAG   (d) 3rd MAG

Fig. 7. Natural data-augmentation produced from the original image with different magnifications. MAG refers to magnification

VI. CONCLUSION AND FUTURE WORK

In this work, we proposed the use of deep learning methods to detect and localize the skin lesions that are trained and tested on the ISBI-2017 challenge dataset. We evaluated the performance of these models on PH2 and a subset of HAM10000 with high accuracy. It is a very challenging task as there are high intra-class variations and inter-class similarities in terms of visual, size, color and appearance in the various skin lesion classes. The Faster-RCNN-InceptionV2 method outperformed the state-of-the-art segmentation model for ROI detection on all testing sets. ROI detection and data augmentation are two important aspects of medical image analysis. We demonstrated the potential of this ROI detection work to propose a natural data-augmentation method that produce the augmentation of skin lesions with different magnification and angles. With natural data-augmentation as a pre-processing step, the performance of state-of-the-art deep learning algorithms for both segmentation and classification tasks have significantly improved. Further, we designed a real-time smartphone application for ROI detection using the light-weight model (SSD-InceptionV2) on an android device attached with a MoleScope. In the future, this work can be extended to train deep learning models to combine both classification and localization ground truths for multi-class skin lesion detection for the diagnosis of different types of skin cancer.

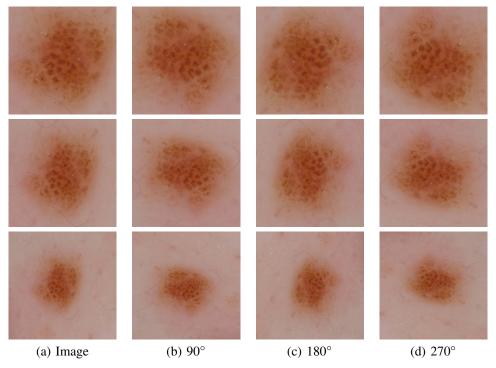(a) Image   (b) 90°   (c) 180°   (d) 270°

Fig. 8. Natural data-augmentation of different angles produced from the images (different magnification)
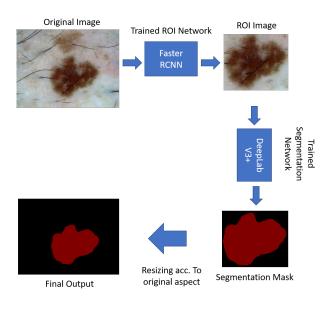

Fig. 9. Segmentation results produced using ROI detection as pre-processing and DeeplabV3+ using natural data-augmentation on ISIC-2017 testing set.

REFERENCES

[1] S. C. Foundation, "Skin cancer facts and statistics," Online, Jan. 2017. [Online]. Available: https://www.skincancer.org/skin-cancer-information/skin-cancer-facts#general

[2] G. Pellacani and S. Seidenari, "Comparison between morphological parameters in pigmented skin lesion images acquired by means of epi-luminescence surface microscopy and polarized-light videomicroscopy," *Clinics in dermatology*, vol. 20, no. 3, pp. 222–227, 2002.

[3] J. Mayer, "Systematic review of the diagnostic accuracy of dermatoscopy in detecting malignant melanoma." *The Medical Journal of Australia*, vol. 167, no. 4, pp. 206–210, 1997.
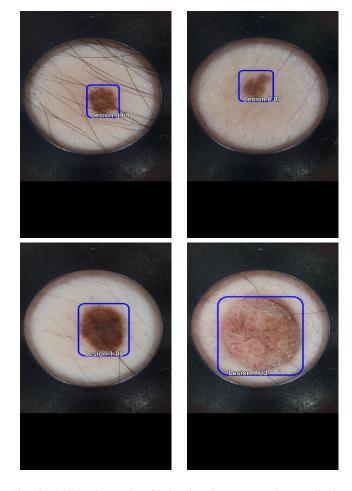

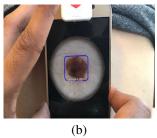Fig. 10. Additional examples of lesion detection on smart-phone application

Fig. 11. Illustration of our real-time ROI detection application on skin lesions: (a) an Android smart-phone with a MoleScope; and (b) Real-time inference with confidence level of 100%.

[4] M. E. Celebi, H. Iyatomi, G. Schaefer, and W. V. Stoecker, "Lesion border detection in dermoscopy images," *Computerized medical imaging and graphics*, vol. 33, no. 2, pp. 148–153, 2009.

[5] C. Barata, M. E. Celebi, and J. S. Marques, "A survey of feature extraction in dermoscopy image analysis of skin cancer," *IEEE journal of biomedical and health informatics*, vol. 23, no. 3, pp. 1096–1109, 2018.

[6] M. E. Celebi, N. Codella, and A. Halpern, "Dermoscopy image analysis: overview and future directions," *IEEE journal of biomedical and health informatics*, vol. 23, no. 2, pp. 474–478, 2019.

[7] N. C. Codella, D. Gutman, M. E. Celebi, B. Helba, M. A. Marchetti, S. W. Dusza, A. Kalloo, K. Liopyris, N. Mishra, H. Kittler *et al.*, "Skin lesion analysis toward melanoma detection: A challenge at the 2017 international symposium on biomedical imaging (isbi), hosted by the international skin imaging collaboration (isic)," in *Biomedical Imaging (ISBI 2018), 2018 IEEE 15th International Symposium on*. IEEE, 2018, pp. 168–172.

[8] ——, "Skin lesion analysis toward melanoma detection: A challenge at the 2017 international symposium on biomedical imaging (isbi), hosted by the international skin imaging collaboration (isic)," *arXiv preprint arXiv:1710.05006*, 2017.

[9] M. Goyal, N. Reeves, S. Rajbhandari, and M. H. Yap, "Robust methods for real-time diabetic foot ulcer detection and localization on mobile devices," *IEEE journal of biomedical and health informatics*, 2018.

[10] A. Criminisi, D. Robertson, E. Konukoglu, J. Shotton, S. Pathak, S. White, and K. Siddiqui, "Regression forests for efficient anatomy detection and localization in computed tomography scans," *Medical image analysis*, vol. 17, no. 8, pp. 1293–1303, 2013.

[11] M. H. Yap and H. T. Ewe, "Region of interest (roi) detection in ultra-sound breast images," in *Proceedings of MMU International Symposium on Information and Communications Technologies (M2USIC)*, 2005, pp. 5–8.

[12] M. Goyal and M. H. Yap, "Multi-class semantic segmentation of skin lesions via fully convolutional networks," *arXiv preprint arXiv:1711.10449*, 2017.

[13] P. Tschandl, C. Rosendahl, and H. Kittler, "The ham10000 dataset, a large collection of multi-source dermatoscopic images of common pigmented skin lesions," *Scientific data*, vol. 5, p. 180161, 2018.

[14] T. Mendonça, P. M. Ferreira, J. S. Marques, A. R. Marcal, and J. Rozeira, "Ph 2-a dermoscopic image database for research and benchmarking," in *Engineering in Medicine and Biology Society (EMBC), 2013 35th Annual International Conference of the IEEE*. IEEE, 2013, pp. 5437–5440.

[15] J. Huang, V. Rathod, C. Sun, M. Zhu, A. Korattikara, A. Fathi, I. Fischer, Z. Wojna, Y. Song, S. Guadarrama *et al.*, "Speed/accuracy trade-offs for modern convolutional object detectors," *arXiv preprint arXiv:1611.10012*, 2016.

[16] S. Ren, K. He, R. Girshick, and J. Sun, "Faster r-cnn: Towards real-time object detection with region proposal networks," in *Advances in neural information processing systems*, 2015, pp. 91–99.

[17] W. Liu, D. Anguelov, D. Erhan, C. Szegedy, S. Reed, C.-Y. Fu, and A. C. Berg, "Ssd: Single shot multibox detector," in *European conference on computer vision*. Springer, 2016, pp. 21–37.

[18] C. Szegedy, V. Vanhoucke, S. Ioffe, J. Shlens, and Z. Wojna, "Rethinking the inception architecture for computer vision," in *Proceedings of the IEEE Conference on Computer Vision and Pattern Recognition*, 2016, pp. 2818–2826.

[19] L.-C. Chen, G. Papandreou, I. Kokkinos, K. Murphy, and A. L. Yuille, "Deeplab: Semantic image segmentation with deep convolutional nets, atrous convolution, and fully connected crfs," *IEEE transactions on pattern analysis and machine intelligence*, vol. 40, no. 4, pp. 834–848, 2018.

[20] M. Goyal, N. D. Reeves, S. Rajbhandari, J. Spragg, and M. H. Yap, "Fully convolutional networks for diabetic foot ulcer segmentation," *arXiv preprint arXiv:1708.01928*, 2017.

[21] Y. Yuan, M. Chao, and Y.-C. Lo, "Automatic skin lesion segmentation using deep fully convolutional networks with jaccard distance," *IEEE Transactions on Medical Imaging*, 2017.

[22] O. Ronneberger, P. Fischer, and T. Brox, "U-net: Convolutional networks for biomedical image segmentation," in *International Conference on Medical Image Computing and Computer-Assisted Intervention*. Springer, 2015, pp. 234–241.

[23] J. Long, E. Shelhamer, and T. Darrell, "Fully convolutional networks for semantic segmentation," in *Proceedings of the IEEE Conference on Computer Vision and Pattern Recognition*, 2015, pp. 3431–3440.

[24] V. Badrinarayanan, A. Handa, and R. Cipolla, "Segnet: A deep convolutional encoder-decoder architecture for robust semantic pixel-wise labelling," *arXiv preprint arXiv:1505.07293*, 2015.

[25] K. He, G. Gkioxari, P. Dollár, and R. Girshick, "Mask r-cnn," in *Proceedings of the IEEE international conference on computer vision*, 2017, pp. 2961–2969.

Michael Shell Biography text here.

PLACE
PHOTO
HERE

John Doe Biography text here.

Jane Doe Biography text here.